

AutoDipole

– Automated generation of dipole subtraction terms –

K. Hasegawa^a, S. Moch^b and P. Uwer^a

^a *Institut für Physik, Humboldt-Universität zu Berlin,
D-10099 Berlin, Germany*

^b *Deutsches Elektronensynchrotron DESY
Platanenallee 6, D-15738 Zeuthen, Germany*

Abstract

We present an automated generation of the subtraction terms for next-to-leading order QCD calculations in the Catani-Seymour dipole formalism. For a given scattering process with n external particles our Mathematica package generates all dipole terms, allowing for both massless and massive dipoles. The numerical evaluation of the subtraction terms proceeds with MadGraph, which provides Fortran code for the necessary scattering amplitudes. Checks of the numerical stability are discussed.

Program summary

Title of program: AutoDipole

Version: 1.2.3

Catalogue number:

Program summary URL: <http://www-zeuthen.desy.de/~moch/autodipole/> or
<http://www.physik.hu-berlin.de/pep/tools/>

E-mail: kouhei.hasegawa@physik.hu-berlin.de,
sven-olaf.moch@desy.de,
peter.uwer@physik.hu-berlin.de

License: —

Computers: Computers running Mathematica (version 7.0).

Operating system: The package should work on every Linux system supported by Mathematica. Detailed tests have been performed on Scientific Linux as supported by DESY and CERN and on openSUSE and Debian.

Program language: Mathematica and Fortran.

Memory required to execute: Depending on the complexity of the problem, recommended at least 128 MB RAM.

Other programs called: MadGraph (stand-alone version MG_ME_SA_V4.4.30) and HELAS

External files needed: MadGraph (including HELAS library) available under
<http://madgraph.hep.uiuc.edu/> or
<http://madgraph.phys.ucl.ac.be/> or
<http://madgraph.roma2.infn.it/>

Keywords: QCD, NLO computations, dipole formalism, Catani-Seymour subtraction.

Nature of the physical problem: Computation of next-to-leading order QCD corrections to scattering cross sections, regularization of real emission contributions.

Method of solution: Catani-Seymour subtraction method for massless and massive partons [1, 2]; Numerical evaluation of subtracted matrix elements interfaced to MadGraph [3–5] (stand-alone version) using helicity amplitudes and the HELAS library [6, 7] (contained in MadGraph).

Restrictions on complexity of the problem: Limitations of MadGraph are inherited.

Typical running time: Dependent on the complexity of the problem with typical run times of the order of minutes.

1 Introduction

The Large Hadron Collider (LHC) allows us to explore an energy regime far beyond what has been accessible in direct measurements up to now. Operating at the TeV scale it will shed light on the mechanism of electroweak symmetry breaking. The large center-of-mass energy allows the production of new heavy particles — if they exist. It is expected that the results obtained from the LHC will significantly influence our future understanding of nature. The high potential of the LHC in making an important step forward towards a deeper understanding of elementary particle physics comes not for free. Experimentally as well theoretically the LHC is a very challenging experiment. The large multiplicity in the individual event together with pile-up and the complications due to the underlying event make the experimental analysis at the LHC highly non-trivial. The separation of known Standard Model (SM) physics from new physics is very demanding, in particular since in many cases the new physics signals are overwhelmed by the large SM backgrounds. Sophisticated methods have been devised in the past to cope with this situation within the experiments with respect to theoretical predictions.

Colliding protons at LHC interact primarily through strong interactions and Quantum Chromodynamics (QCD) plays an important role in this context. It is well known that perturbative QCD predictions are in general plagued by a large (residual) renormalization and factorization scale dependence. It is not rare that predictions for cross sections change by 100% when the scales are varied in a reasonable range. To reduce the large scale uncertainty next-to-leading order (NLO) calculations are required, which generally consist of two ingredients: one contribution from the virtual corrections and a second contribution from real emission of one additional parton. With respect to the virtual contributions much progress has been achieved recently, although the evaluation of one-loop amplitudes for “large” multiplicities ($2 \rightarrow 3$, $2 \rightarrow 4$) is still a highly non-trivial enterprise. Fortunately, as far as the real corrections are concerned the situation is much better and efficient methods exist for the numerical evaluation of the required matrix elements. However, the integral over the phase space leads to soft and collinear singularities, which we denote here generically as infrared (IR) divergencies. In combination with the virtual corrections, all IR cancel between the two contributions for the physical observables of interest [8–10].

General algorithms, typically classified either as slicing or subtraction methods, are available for the extraction of soft and collinear singularities encountered in the real corrections. In both cases one makes use of the universal behavior of QCD amplitudes for soft and collinear configurations. IR singularities are nowadays usually regulated within dimensional regularization, so the same regulator has to be applied to the real corrections in a way that numerical integration over the phase space in 4 dimensions is possible in the end.

In slicing methods the idea is to separate the phase space into *resolved* and *unresolved* contributions [11–14]. Unresolved regions at NLO are those where one parton becomes soft or two become collinear. In these regions the matrix elements are approximated using the QCD factorization theorems. After this simplification the unresolved regions can be integrated analytically in $d = 4 - 2\epsilon$ dimensions and the emerging singularities cancel analytically against the corresponding ones in the virtual corrections. Resolved regions on the other hand exclude all IR singularities by definition and can be integrated numerically in 4 dimensions. A one-dimensional illustration of the slicing approach is shown below,

$$\int_0^1 \frac{f(x)}{x^{1-\epsilon}} dx \approx f(0) \int_0^\delta \frac{1}{x^{1-\epsilon}} dx + \int_\delta^1 \frac{f(x)}{x} dx + O(\epsilon)$$

$$= \frac{1}{\epsilon} f(0) + \ln(\delta) f(0) + \int_{\delta}^1 \frac{f(x)}{x} dx + O(\epsilon), \quad (1.1)$$

where $f(x)$ is an arbitrary function, which is regular at $x = 0$. It is a drawback of the slicing method that partial results exhibit a logarithmic dependence on the cut δ which separates resolved from unresolved configurations. This logarithm — which cancels when the two parts (resolved and unresolved) are combined — is manifest in the analytic integration of the unresolved terms. However, for the resolved terms the logarithmic dependence arises from the numerical phase space integration. Since the matrix elements in the unresolved phase space regions are only approximate one tends to make the respective region around singular configurations as small as possible. This procedure, though, would result in large numerical cancellations and a loss of accuracy in the sum of the resolved and unresolved parts compared to the accuracy reached in the numerical integration. In practice this requires a compromise between the quality of the approximation and the numerical effort to achieve a certain precision in the sum of both, resolved and unresolved contributions. Subtraction methods make use of our knowledge about QCD factorization in the soft and collinear limits to construct suitable “counter-terms”. These have to match pointwise all singularities in the real-emission matrix elements and, at the same time, should be simple enough to be integrated analytically in $d = 4 - 2\epsilon$ dimensions over the entire phase space [1, 2, 15]. A one-dimensional example is shown in Eq. (1.2).

$$\begin{aligned} \int_0^1 \frac{f(x)}{x^{1-\epsilon}} dx &= \int_0^1 \frac{f(x) - f(0)}{x} dx + f(0) \int_0^1 \frac{1}{x^{1-\epsilon}} dx + O(\epsilon) \\ &= \int_0^1 \frac{f(x) - f(0)}{x} dx + \frac{1}{\epsilon} f(0) + O(\epsilon). \end{aligned} \quad (1.2)$$

Here the cancellation of the singularity takes place at the integrand level — i.e. the divergencies cancel pointwise — and the integrals are easier to evaluate numerically. However, care must be taken with respect to the numerical accuracy. Deep in the singular regions the individual contributions become arbitrary large and, due to limited numerical precision of floating point arithmetic, their cancellation might be incomplete leading to potentially wrong results. While our one-dimensional example in Eq. (1.2) admits the construction of a suitable subtraction term in a straightforward manner this no longer true when considering complicated scattering amplitudes. Fortunately, this formidable problem has been solved with the Catani-Seymour dipole formalism [1, 2]. (Similar algorithms are presented in Refs. [15, 16].) Based on the factorization of soft and collinear singularities in an $SU(N)$ gauge theory all subtraction terms are constructed from universal functions and process specific amplitudes. It turns out, though, that for complicated processes the complete subtraction term is a sum over many different contributions — tedious to derive by hand. On the other hand, the method is completely algorithmic, thus an automation is feasible. This is a timely problem and its solution is the aim of the present work [17, 18]. We note that it has recently also been addressed by other groups [19–22], see also [23].

In passing let us briefly mention that the attractive features of the subtraction approach (universality of counter-terms and numerical stability) have led to extensions of the formalism to next-to-next-to-leading order (NNLO), see e.g. [24–27]. Presently, the proposed schemes at NNLO apply to processes without colored partons in the initial state and an arbitrary number of massless particles (colored or colorless) in the final state. The necessary counter-terms are either derived from so-called antenna functions [28] or alternatively defined as universal counter-terms based on QCD

factorization in the various soft and collinear limits of singly- and double-unresolved parton configurations [29–32]. Ongoing work at NNLO is concerned with extensions to colored partons in the initial state as needed for the LHC.

The outline of the paper is as follows. In Section 2 we review the general features of the Catani-Seymour algorithm [1, 2] and in Section 3 we describe the details of its implementation in the AutoDipole package. Particular emphasis is put on the details of the numerical evaluation of subtraction terms via an interface to MadGraph [3–5], which uses the HELAS library [6, 7] for the computation of helicity amplitudes. Section 4 illustrates with a few examples of how to use AutoDipole in practice. The examples serve also as a non-trivial cross check of the implementation when compared with existing results from the literature. Finally, we conclude in Section 5 and list some technical details of the implementation and the comparison with the literature in Appendices A–C.

2 Review of the Catani-Seymour subtraction formalism

We consider a generic scattering process for the production of an n -parton final state. At NLO accuracy in QCD the corresponding cross section may be written as:

$$\sigma_{\text{NLO}} = \sigma_{\text{LO}} + \delta\sigma_{\text{NLO}}, \quad (2.1)$$

where σ_{LO} denotes the Born contribution at leading order (LO) and the genuine NLO correction $\delta\sigma_{\text{NLO}}$ receives contributions from three different sources,

$$\delta\sigma_{\text{NLO}} = \int_n d\sigma_{\text{virt}} + \int_{n+1} d\sigma_{\text{real}} + \int dx \int_n d\sigma_{\text{fact}}. \quad (2.2)$$

By $d\sigma_{\text{virt}}$ we denote here the contributions from the virtual corrections and by $d\sigma_{\text{real}}$ the ones from the real emission of one additional parton. For hadrons in the initial state there is a third contribution $d\sigma_{\text{fact}}$ due to the factorization of initial state singularities. The subscript on the integral signs in Eq. (2.2) indicates the dimensionality of the phase space: The virtual corrections are integrated over an n -parton phase space while the real emissions are integrated over an $(n+1)$ -parton phase space. All three contributions are individually divergent and thus require regularization in intermediate steps until the divergencies are canceled. In the Catani-Seymour formalism the expression for $\delta\sigma_{\text{NLO}}$ in Eq. (2.2) is rewritten schematically:

$$\delta\sigma_{\text{NLO}} = \int_{n+1} (d\sigma_{\text{real}} + dA) + \int_n (d\sigma_{\text{virt}} + \int_1 dA') + \int dx \int_n (d\sigma_{\text{fact}} + dA''), \quad (2.3)$$

with

$$0 = \int_{n+1} dA + \int_n \int_1 dA' + \int dx \int_n dA''. \quad (2.4)$$

The expressions dA , dA' and dA'' are defined such that they render the individual pieces in Eq. (2.3) finite. In the Catani-Seymour formalism, they correspond to the sum of all dipoles (dA), the integrated dipoles ($\int_1 dA'$), **I**-term, and the terms arising from mass factorization (dA'') including the so-called **P**-, **K**- and **H**-terms.

The explicit form of dA is constructed from the knowledge about the soft and collinear factorization of QCD amplitudes, which exhibit a simple factorization for collinear configurations. The

expression for dA in Eq. (2.3) is obtained as a sum over potentially collinear partons since the factorization for soft configurations can be derived from the collinear behavior of the amplitudes. For soft singularities however only color-ordered amplitudes exhibit a simple factorization, which implies in general non-trivial color correlations at the level of the squared matrix elements. These color correlations are reflected by the reference to an additional (so-called) spectator parton. The subtraction dA is thus written as a sum of individual dipoles in the following form:

$$dA = \sum \mathcal{D}(i, j; k), \quad (2.5)$$

where the sum runs over all colored partons in scattering process and the possible configurations for $\{i, j; k\}$ are determined from the real corrections for which the subtraction term is constructed. The generic form of the dipoles is given by

$$\mathcal{D}(i, j; k) = d_{ij} \times \langle 1, \dots, \tilde{i}j, \dots, \tilde{k}, \dots, n | \mathbf{V}_{ij,k} | 1, \dots, \tilde{i}j, \dots, \tilde{k}, \dots, n \rangle. \quad (2.6)$$

The singular behavior is contained in the pre-factor d_{ij} which is essentially the intermediate propagator before the splitting into $i + j$. The bra ($\langle \dots |$) and ket ($| \dots \rangle$) notation for the amplitude is used since it appears as a vector in color and spin space. Accordingly $\mathbf{V}_{ij,k}$ acts as an operator in color and spin space and introduces the non-trivial color and spin correlations mentioned above.

As a concrete example we display the expression for $\mathcal{D}(g_i, g_j, k)$ with all three partons in the final state, i.e.

$$\mathcal{D}(g_i, g_j, k) = -\frac{1}{2p_i \cdot p_j} \langle 1, \dots, \tilde{i}j, \dots, \tilde{k}, \dots, n | \frac{\mathbf{T}_k \cdot \mathbf{T}_{ij}}{\mathbf{T}_{ij}^2} V_{g_i g_j, k} | 1, \dots, \tilde{i}j, \dots, \tilde{k}, \dots, n \rangle. \quad (2.7)$$

$\mathcal{D}(g_i, g_j, k)$ describes the situation of a collinear splitting of the gluons i and j (emitter pair) in the presence of a spectator parton k . Here, the \mathbf{T}_i are the color charge operators depending on the partons being in the fundamental or adjoint representation of the color SU(3) (for details we refer to [1, 2]). The function $V_{g_i g_j, k}$ is given by

$$\begin{aligned} V_{g_i g_j, k}^{\mu\nu} &= \langle \mu | V_{g_i g_j, k} | \nu \rangle \\ &= 16\pi\alpha_s \mu^{2\epsilon} C_A \left[-g_{\mu\nu} \left(\frac{1}{1 - z_i(1 - y_{ij,k})} + \frac{1}{1 - z_j(1 - y_{ij,k})} - 2 \right) \right. \\ &\quad \left. + (1 - \epsilon) \frac{1}{p_i \cdot p_j} (z_i p_i^\mu - z_j p_j^\mu)(z_i p_i^\nu - z_j p_j^\nu) \right], \end{aligned} \quad (2.8)$$

where z_i and $y_{ij,k}$ are some functions of the Lorentz scalars s_{ij} , s_{ik} , and s_{jk} and α_s is the strong coupling. The quantity,

$$\langle 1, \dots, \tilde{i}j, \dots, \tilde{k}, \dots, n | \mathbf{T}_k \cdot \mathbf{T}_{ij} | 1, \dots, \tilde{i}j, \dots, \tilde{k}, \dots, n \rangle, \quad (2.9)$$

is called the color linked Born amplitude squared (CLBS). The amplitude ($| \dots \rangle$) is deduced from the real emission by the factorization of one splitting. The color factor is extended by two color operator insertion, $\mathbf{T}_k \cdot \mathbf{T}_{ij}$. The CLBS has the reduced kinematics as input. In the example the original momenta (p_i, p_j, p_k) are reduced to $(\tilde{p}_{ij}, \tilde{p}_k)$ where for example, the \tilde{p}_{ij} is defined as

$$\tilde{p}_{ij}^\mu = p_i^\mu + p_j^\mu - \frac{y_{ij,k}}{1 - y_{ij,k}} p_k^\mu. \quad (2.10)$$

Generally, $(n + 3)$ original momenta are reduced to the $(n + 2)$ momenta in each dipole term. One distinguished feature of the dipole subtraction is that the reduced kinematics satisfy the on-shell conditions and momentum conservation, which makes it possible to evaluate the reduced Born amplitude by existing codes for LO calculations. In the gluon emitter case like the example above, the second term in the square bracket in Eq. (2.8) introduces spin correlations of the gluon. In that case we need also to evaluate the CLBS where the helicity of the emitter gluon in the amplitude is different from the one in the conjugate. In the next section we explain how the three main ingredients, the generation of the dipole terms, the CLBS, and the dipoles with a gluon emitter, are implemented in our package.

The other two functions $\int_1 dA'$ and dA'' in Eq. (2.3) are easily explained. The first one ($\int_1 dA'$) denotes the integrated dipoles which cancel the corresponding IR divergencies in the virtual contributions at NLO. They can be constructed from universal insertion operators \mathbf{I} , to be sandwiched between the bra ($\langle \dots |$) and ket ($| \dots \rangle$) amplitudes of the corresponding Born process, i.e. in the reduced kinematics with $(n + 2)$ momenta. The expressions for the \mathbf{I} -terms depend on the parton type, e.g. for massless partons we have

$$\mathbf{I}(\{p\}, \epsilon) = -\frac{\alpha_s}{2\pi} \frac{1}{\Gamma(1-\epsilon)} \sum_i \frac{1}{\mathbf{T}_{ij}^2} \mathcal{V}_i(\epsilon) \sum_{j \neq i} \mathbf{T}_i \cdot \mathbf{T}_j \left(\frac{4\pi\mu^2}{2p_i \cdot p_j} \right)^\epsilon, \quad (2.11)$$

where the sum runs over all parton momenta $\{p\}$ in the Born kinematics (corresponding also to the NLO virtual corrections). The poles in dimensional regularization are contained in the function \mathcal{V}_i , that is $\mathcal{V}_i(\epsilon) \sim 1/\epsilon^2$ and $\sim 1/\epsilon$ for massless partons [1]. For massive partons [2], the corresponding function $\mathcal{V}_i(\epsilon, m_i, m_j)$ contains single poles $\mathcal{V}_i(\epsilon, m_i, m_j) \sim 1/\epsilon$ from soft gluons and the \mathcal{V}_i depend logarithmically on the parton masses m_i which screen the collinear singularity, see also [16, 33]. The formulation suggested in [2] (and used in AutoDipole) allows for a smooth interpolation in the limit $m_i \rightarrow 0$. The color operator insertions, $\mathbf{T}_i \cdot \mathbf{T}_j$, lead again to non-trivial color correlations and require the evaluation of the same CLBS in Eq. (2.9) with the phase space of n final state partons. The last term in Eq. (2.3) (dA'') abbreviates the so-called \mathbf{P} -, \mathbf{K} - and \mathbf{H} -terms. They are needed for mass factorization of initial state singularities in hadron collisions to be absorbed in renormalized parton distributions and, likewise, also for the final-state singularities in processes with identified hadrons giving rise to scale dependence of the fragmentation functions. For instance in the case of initial state divergencies the \mathbf{P} -operator takes the following form

$$\mathbf{P}^{a,b}(\{p\}, x, \mu_F^2) = \frac{\alpha_s}{2\pi} P^{ab}(x) \frac{1}{\mathbf{T}_b^2} \sum_{i \neq b} \mathbf{T}_i \cdot \mathbf{T}_b \ln \frac{\mu_F^2}{2xp_a \cdot p_i}, \quad (2.12)$$

where μ_F is the factorization scale and P^{ab} are the standard (space-like) LO splitting functions containing the well-known '+'-distributions in their diagonal components. Like the \mathbf{I} -operators in Eq. (2.11), the \mathbf{P} -operators act on the amplitudes of the corresponding Born process, leading to color correlations and giving rise to the CLBS as in Eq. (2.9). Here the dependence of \mathbf{P} in Eq. (2.12) on the parton momentum fraction x leads to convolutions when integrated with the Born squared matrix elements or CLBS, see Eq. (2.3), and the implementation needs a prescription for '+'-distributions (see e.g. Eq. (B.26) in [34]).

Similar definitions as in Eq. (2.12) hold for the \mathbf{K} - and \mathbf{H} -operators. They also contain distributions $1/(1-x)_+$ that are singular in the collinear limit and parametrize the factorization scheme

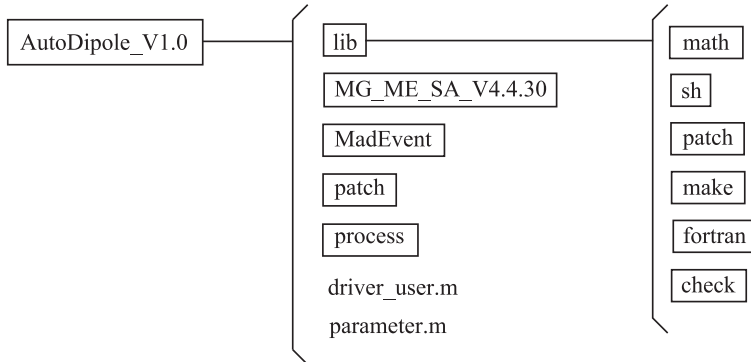


Figure 1: The directory structure of the AutoDipole package.

dependence, \mathbf{K} for factorization in the initial state and \mathbf{H} in the final state. These remarks conclude our brief review of the Catani-Seymour dipole formalism. For details the reader is referred to the original literature [1, 2].

3 The AutoDipole package

The AutoDipole package constructs all necessary subtraction terms of the Catani-Seymour formalism [1, 2] for a given scattering process with n colored partons in a fully automatic manner. It can handle both massless and massive partons and it also allows for additional (non-colored) SM particles in the scattering process, e.g. couplings of quarks to γ , Z -, W^\pm -bosons and so on.

Let us briefly sketch the details of our implementation of the dipole subtraction formalism, because there is a large freedom in the way how this can be performed. For instance, in Refs. [35, 36] the implementation was realized in form of two independent C/C++ libraries providing all the necessary functions to evaluate the dipole terms. As a slight disadvantage of this approach the produced code is non-local and that there is some redundancy in the calculation. In the present work we follow a different strategy. The main idea here is to have a code generator which will produce an optimized flat code. To realize this we have constructed a Mathematica program which acts as such a generator and its output is interfaced with MadGraph [3–5]. To that end we found the stand-alone version of MadGraph suitable and for the numerical evaluation of all subtraction terms, we use helicity amplitudes provided by MadGraph (which are based on the HELAS library [6, 7]).

3.1 Structure of the code

The complete layout of the code of the AutoDipole package is displayed in Figure 1. The major part of the source code in the package (all contained in the directory `lib`) is written in Mathematica. This includes all algorithms for the generation of the dipole terms as well as the evaluation of the \mathbf{I} -, \mathbf{P} - and \mathbf{K} -operator insertions sandwiched between the Born amplitudes in the appropriate kinematics. The use of a computer algebra program like Mathematica has the clear advantage here that all terms are accessible to symbolic manipulation. This feature is very useful for general studies of the IR behavior of scattering amplitudes.

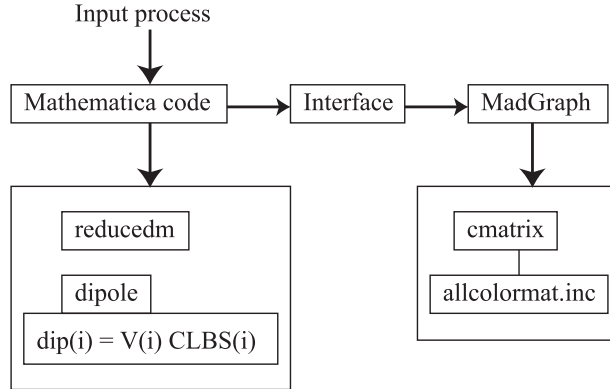


Figure 2: The flowchart of the execution of AutoDipole.

In using AutoDipole we are primarily interested in the generation of Fortran code for all subtraction terms of Eq. (2.3). The essential parts of the flowchart are displayed in Figure 2. From a given input process, the Mathematica code generates all dipole terms. The important files here are `dipole.f`, `reducedm.f`, and the shell script for the interface with MadGraph, where `dipole.f` contains all dipole terms except for the reduced kinematics and the CLBS. The routine `reducedm.f` calculates the reduced kinematics of each dipole term as defined in Eq. (2.10). The subsequent run of a patched version of MadGraph (contained in the directory `patch`) via the interface produces the files, `cmatrix.f` and `allcolormat.inc`. The routine `cmatrix.f` evaluates all CLBS as in Eq. (2.9). It includes the file `allcolormat.inc`, which contains all extended color matrices by the two color operator insertions. We use the latest version of MadGraph (MG_ME_SA_V4.4.30). All the process specific Fortran files mentioned above are stored in a new directory under `process`, see Figure 1.

In short, the evaluation of the generated Fortran code for the dipole terms proceeds along the following chain, see Figure 2. The routine `reducedm.f` receives a given phase space point as input and calculates the reduced kinematics of each dipole term. Next, the routine `cmatrix.f` (with the reduced kinematics as input) computes the CLBS of each dipole term together with the extended color matrices in `allcolormat.inc`. Finally the routine `dipole.f` returns the values of all dipole terms having received the reduced kinematics and the CLBS as input. All this is done automatically when the user executes the command `./runD` (see Sections 4.2 and 4.3) to calculate the subtraction term for a specific phase space point.

The algorithm of dipole term generation by the Mathematica code is shown in Section 3.2. A detailed account of the calculation of the CLBS is given in Section 3.3 and some aspects of the spin correlations for the particular case of a gluon emitter are presented in Section 3.4. The check of IR safety is explained in Section 3.5. An explanation of how to run AutoDipole is deferred to Section 4.

3.2 Algorithm of dipole generation

Let us start with a short description of the Mathematica code generating all dipole terms. This procedure makes use of the following three steps:

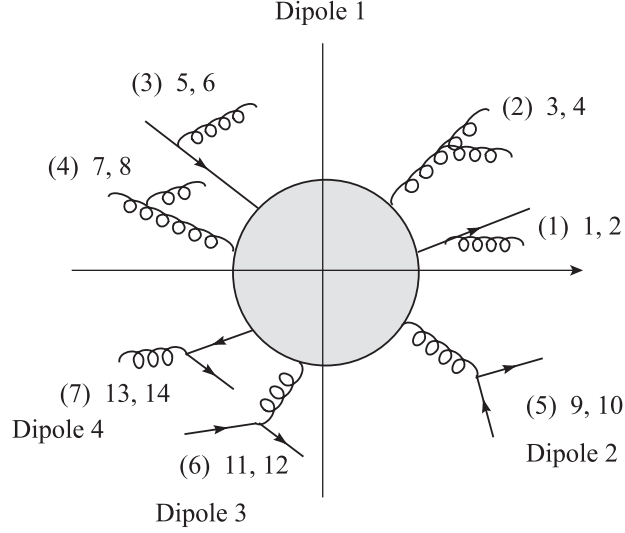


Figure 3: The four categories of dipoles (Dipole 1, ..., 4), the seven possible splittings and their order of creation in AutoDipole, see Table 2 for details.

1. Choose all possible emitter pairs from the external legs.

For a given real emission $2 \rightarrow (n + 1)$ -particle scattering process we abbreviate the set of initial (final) state partons collectively as $\{\text{initial}\}$ ($\{\text{final}\}$), i.e. the scattering reaction reads generically

$$\{\text{initial}\} \rightarrow \{\text{final}\}. \quad (3.1)$$

Then, the first step in the construction of the dipoles is the choice of the emitter pair, that is the root of the splitting of the quarks and gluons. This also specifies the kind of splitting. At NLO in QCD, there exist seven possible splittings, which we group into four classes and we enumerate these types of dipoles accordingly, Dipole 1, ..., and Dipole 4. The ordering is shown in Figure 3. Due to the factorization of the splitting each dipole is associated to a certain reduced Born process and the following equations show schematically the operations performed on the sets of partons in Eq. (3.1) in order to construct the corresponding reduced Born process,

$$\text{Dipole 1: } \{\text{initial}\} \rightarrow \{\text{final}\} - g, \quad (3.2)$$

$$\text{Dipole 2: } \{\text{initial}\} \rightarrow \{\text{final}\} - f\bar{f} + g, \quad (3.3)$$

$$\text{Dipole 3: } \{\text{initial}\} - f + g \rightarrow \{\text{final}\} - f, \quad (3.4)$$

$$\text{Dipole 4: } \{\text{initial}\} - g + \bar{f} \rightarrow \{\text{final}\} - f, \quad (3.5)$$

where g is a gluon and $f(\bar{f})$ a quark (anti-quark). The notation in Eqs. (3.2)–(3.5) indicates which partons are removed from or added to the respective sets $\{\text{initial}\}$ and $\{\text{final}\}$. The cases Dipole 3 and 4 can also occur with a reduced Born cross section where f and \bar{f} are exchanged. The groups Dipole 2, 3 and 4 also need to account for the existence of various quark flavors, i.e. they exhibit manifest flavor dependence, see Table 2 for details.

2. Choose all possible spectators for each emitter pair.

The spectator is one external field which is different from both fields of the emitter pair and its choice is a purely combinatorial procedure. We use indices, i, j , and k , for fields in a final state

and, respectively, indices, a and b , for an initial state field. For a spectator in the final (initial) state denoted by k (b), this condition means $k \neq i, j$ ($b \neq a$). It emerges from a special feature of the subtraction formalism namely that the squared matrix elements with the Casimir operator, $\langle \mathbf{T}_i^2 \rangle$, is expressed, due to color conservation, through CLBS $\langle \mathbf{T}_i \cdot \mathbf{T}_k \rangle (i \neq k)$ which always includes one color dipole configuration in the part.

3. Construct the dipole terms from the chosen combinations of emitter and spectator.

The previous steps provide all such combinations as pairings of the type (emitter, spectator) = $(ij, k), (ij, b), (ai, k)$, and (ai, b) . Each case corresponds to one dipole term, for which we use the short-hands $D_{ij,k}, D_{ij}^a, D_k^{ai}$, and $D^{ai,b}$, respectively. Detailed information about all pairings of emitter and spectator as well as the potential presence of a mass parameter is given in Table 2 in Appendix A. For explicit expressions we refer to [1, 2].

Here it is worth to stress a few points. First of all, the chosen order for the generation has the advantage of grouping together the reduced Born matrix elements. The CLBS in the same category exhibit the same Lorentz structure, only the extended color matrix is different. This ordering leads to a block-diagonal structure in the evaluation of the color correlations. It leads to flat Fortran code including higher readability. Additionally, for the category Dipole 1 the Casimir operator \mathbf{T}_{ij}^2 in the denominator always cancels against the same one in the dipole splitting function. This cancellation leads to manifest simplifications. Finally, in our set-up we have access to the symbolic expression and can easily identify or extract partial subsets of dipole terms, if needed. For example we may want to discard the $t - \bar{t}$ (heavy-quark) splitting in the category Dipole 2, because this splitting does not give rise to poles in ϵ . Our way of generating the dipoles in the package easily allows this selection. The user can discard dipoles of a specific category in the input file `parameter.m` (see Section 4).

At this stage it remains to discuss the generation of all terms involving the **I**-, **P**- and **K**-operators. This is sketched in Figure 4. Given, that these operators originate from the phase space integral over unresolved parton of the dipole terms, it is clear that we only need a subset of all previously generated terms. From all reduced Born amplitudes generated for the regularization of the real emission contributions (i.e. Figure 3) we need only the CLBS in the category Dipole 1 for all **I**-, **P**-, and **K**-operator insertions. Hence, no new information is required and the Mathematica package assembles the respective expressions (along with the color correlations, see Section 3.3) in the Fortran files `Iterm.f` and `PKterm.f`.

3.3 The color linked Born amplitude squared

The numerical evaluation of Born amplitudes (or their squares) is a routine task for many publicly available packages designed for automated LO calculations. As announced above, we choose the stand-alone version of MadGraph [3–5] for this purpose and the added feature needed is the evaluation of the color link operators, see e.g. Eq. (2.7). This can be done by a patch and allows us to obtain all CLBS in an automatic way, see Figure 2.

The generation of the amplitudes in MadGraph proceeds via Feynman diagrams and the color factors are separated from each diagram. During the evaluation everything is expressed in terms of generators of the fundamental representation of the color SU(3). A typical example is that the factor f^{abc} of the gluon three-point vertex is rewritten in terms of the fundamental generator t_{ij}^a

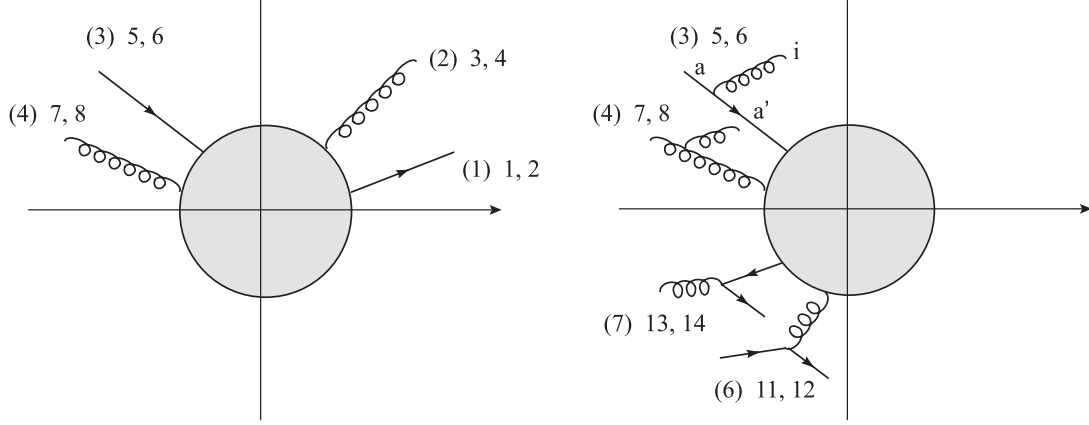


Figure 4: The order of creation of the integrated dipoles in AutoDipole with insertion of the **I**-operator (left) and of the **P**- and **K**-operators (right), see Tables 3 and 4 for details.

with the help of the identity,

$$f^{abc} = -2i(\text{Tr}[t^a t^b t^c] - \text{Tr}[t^c t^b t^a]). \quad (3.6)$$

The color factors of each diagram are sorted in a unique order and they are expressed in a sum. When a specific term of a diagram is identical to one of the other diagrams, both are combined as

$$M = \sum_a C_a J_a, \quad (3.7)$$

where C_a denotes the independent color factors. Each C_a has fundamental and adjoint color indices corresponding to the external quarks and the gluons, respectively. J_a is the joint amplitude, e.g. $J_1 = +A_1 - A_3 + \dots$ where A_i is the partial amplitude of i -th diagram (with the color factor stripped off). The invariant matrix element squared is finally expressed in the form,

$$|M|^2 = (\vec{J})^\dagger \text{CF} \vec{J}, \quad (3.8)$$

where the color matrix CF is defined as

$$(\text{CF})_{ab} = \sum_{\text{color}} C_a^* C_b. \quad (3.9)$$

For the CLBS we need to evaluate Eq. (3.8) with an insertion of two additional color operators to the emitter and spectator legs. This is precisely what our patch of MadGraph does (see Figure 1 and the directory `lib/patch`). The subroutines of MadGraph for the color factor calculations are well structured and the original routines to add the color factors t_{ij}^a and f^{abc} can be applied to the additional color insertions for the CLBS. The color algebra of the $\text{SU}(3)$ is performed numerically and the resulting extended color matrix CF is written to the file `allcolormat.inc`, see Figure 2. We have realized the two color operator insertions for all CLBS in an automatic way and we have also checked that MadGraph with our interface works for a set of rather involved processes. As a simple example let us discuss the color insertions required for the process $g(a)g(b) \rightarrow u(1)\bar{u}(2)g(3)$.

The reduced Born process $g(a)g(b) \rightarrow u(1)\bar{u}(2)$ has three diagrams and the color factors are combined into two independent ones, $(C_1, C_2) = ((t^a t^b)_{12}, (t^b t^a)_{12})$. The components of the color matrix are given by the traces, $(CF)_{11} = (CF)_{22} = \text{Tr}[t^b t^a t^a t^b]$ and $(CF)_{12} = (CF)_{21} = \text{Tr}[t^b t^a t^b t^a]$. Then the color matrix is calculated as

$$CF = \begin{pmatrix} 16/3 & -2/3 \\ -2/3 & 16/3 \end{pmatrix}. \quad (3.10)$$

In the CLBS we need for instance the fundamental operator insertions into the legs 1 and 2. The components of the color matrix CF are modified to $(CF')_{11} = \text{Tr}[t^b t^a t^c t^a t^b t^c]$ and $(CF')_{12} = \text{Tr}[t^b t^a t^c t^b t^a t^c]$. Then the modified color matrix is obtained as

$$CF' = \begin{pmatrix} 1/9 & 10/9 \\ 10/9 & 1/9 \end{pmatrix}. \quad (3.11)$$

One of the more complicated examples consists of the two color operator insertions into the process $g(a)g(b) \rightarrow t(1)\bar{t}(2)g(3)g(4)$. In MadGraph the normal SU(3) color matrix for the process is a 24×24 matrix. The first 15 components in the first row read (we refrain from spelling out the rest),

$$CF = \frac{1}{54}(512, 8, -64, 80, 8, -10, -1, -64, -64, 8, -1, -10, -1, 62, -10, \dots). \quad (3.12)$$

Upon insertions of two adjoint color operators for a gluon into the legs 3 and 4 the extended routines calculate the modified color matrix as

$$CF' = \frac{1}{4}(8, 0, 8, 16, 0, -2, 0, 8, -1, -1, 1, 2, -8, -7, 1, \dots), \quad (3.13)$$

and, of course, the result in Eq. (3.13) agrees with independent checks.

3.4 Spin correlations for gluon emitters

As we have seen above the dipoles for the splittings $g \rightarrow gg$ and $g \rightarrow q\bar{q}$ (which involve a gluon emitter) introduce spin correlations (see e.g. Eq. (2.7)). Since our numerical evaluation of the reduced Born amplitudes uses helicity amplitudes, we have to derive the components of the tensor for the spin correlations in the helicity formalism as well. To that end, we choose the definitions in [37] which we here call the XZC gluon polarization vector.

Let us illustrate the necessary steps (formulated in [38]) with the case of the massless dipole term $\mathcal{D}(g_i, g_j, k)$ in Eq. (2.7),

$$\mathcal{D}(g_i, g_j, k) = -\frac{1}{2p_i \cdot p_j} V_{g_i g_j, k}^{\mu\nu} \frac{1}{C_A} (A_\mu^* \mathbf{T}_k \cdot \mathbf{T}_{ij} A_\nu), \quad (3.14)$$

where $V_{g_i g_j, k}^{\mu\nu}$ is written schematically as

$$V_{g_i g_j, k}^{\mu\nu} = 16\pi\alpha_s \mu^{2\epsilon} C_A (-C_1 g^{\mu\nu} + C_2 L^\mu L^\nu), \quad (3.15)$$

with $L^\mu = z_i p_i^\mu - z_j p_j^\mu$ and some Lorentz scalars $C_{1,2}$ (e.g. given in Eq. (2.8)). Moreover, in Eq. (3.14) we have expressed the CLBS in Eq. (2.9) through amplitudes A_μ and A_ν , where the

polarization vector $\epsilon_\mu^\lambda(\tilde{p}_{ij})$ of the emitter gluon with momentum \tilde{p}_{ij} has been amputated. Then we can transform both the dipole splitting function $V^{\mu\nu}$ and the amplitude A_μ to a helicity basis by inserting the polarization sum $\sum_\lambda \epsilon_\mu^{\lambda*} \epsilon_\nu^\lambda$ as

$$A_\mu^* V^{\mu\nu} A_\nu = \sum_{\lambda', \lambda} A_{\lambda'}^* V^{\lambda'\lambda} A_\lambda, \quad (3.16)$$

$$V^{\lambda'\lambda} = \epsilon_\mu^{\lambda'*} V^{\mu\nu} \epsilon_\nu^\lambda, \quad (3.17)$$

and we obtain the dipole $\mathcal{D}(g_i, g_j, k)$ in a \pm -helicity basis as

$$\begin{aligned} \mathcal{D}(g_i, g_j, k) &= -\frac{1}{2p_i \cdot p_j} 16\pi\alpha_s \mu^{2\epsilon} \\ &\times \left[(C_1 + C_2 |E_+|^2) (A_+^* \mathbf{T}_k \cdot \mathbf{T}_{ij} A_+ + A_-^* \mathbf{T}_k \cdot \mathbf{T}_{ij} A_-) + 2 C_2 \text{Re} (E_+^* E_- A_+^* \mathbf{T}_k \cdot \mathbf{T}_{ij} A_-) \right]. \end{aligned} \quad (3.18)$$

Here we have used gauge invariance, the on-shell condition for the gluon and orthogonality of the polarization vectors, which gives rise to the relations $\epsilon^{\lambda*} \cdot \tilde{p}_{ij} = A \cdot \tilde{p}_{ij} = L \cdot \tilde{p}_{ij} = \tilde{p}_{ij}^2 = 0$. The quantity E_\pm needed to express the dipoles in a helicity basis is defined as (see e.g. [38])

$$E_\pm = \epsilon_\pm \cdot L. \quad (3.19)$$

As a subtlety, we would like to point out the following. In the HELAS library [6, 7] the gluon polarization vector is calculated by the subroutine `VXXXXX` and taken to be in a helicity basis but the phase conventions are different from the ones in [37]. Thus we have to relate these conventions to our choice [37]. Although it may be natural to use the same definition for the gluon polarization vectors as in HELAS for the dipole splitting functions (e.g. $V_{g_i g_j, k}^{\mu\nu}$ in Eq. (3.15)) we have the freedom not to do so because of gauge invariance and the on-shell condition. In our implementation we have chosen the latter option with the advantage that the calculation of the dipole splitting functions can be completely separated from the part for evaluation of the CLBS. With the XZC definitions E_\pm in Eq. (3.19) is expressible in terms of spinor products which can be easily implemented in Fortran code.

The polarization vectors of HELAS [6, 7] are written in a helicity basis as

$$\epsilon_{\mu[\text{HELAS}]}^\pm(k, q) = \frac{1}{\sqrt{2}} (\mp \epsilon_{\mu(1)} - i \epsilon_{\mu(2)}), \quad (3.20)$$

with the explicit expression for the vectors in a linear basis, $\epsilon_{\mu(1,2)}$ given in [6, 7]. Likewise, for XZC [37] we have

$$\epsilon_{\mu[\text{XZC}]}^+(k, q) = \frac{\langle q - |\gamma_\mu| k - \rangle}{\sqrt{2} \langle qk \rangle^*}, \quad (3.21)$$

where the relation $\epsilon_{\mu[\text{XZC}]}^{\pm*} = \epsilon_{\mu[\text{XZC}]}^\mp$ holds and q is an arbitrary reference momentum. The difference between the conventions Eq. (3.20) and Eq. (3.21) amounts to a complex phase,

$$\epsilon_{[\text{XZC}]}^{\pm*}(k, q) \cdot \epsilon_{[\text{HELAS}]}^\mp(k, q') = \mp e^{\pm i\phi(k)}. \quad (3.22)$$

The phase difference contributes to only the second term in the square bracket in Eq. (3.18) and it is then rewritten as

$$+ 2 C_2 \text{Re} \left(E_+^* E_- A_+^* \mathbf{T}_k \cdot \mathbf{T}_{ij} A_- \right)_{[\text{XZC}]} = -2 C_2 \text{Re} \left(\left(e^{+i\phi(k)} E_+ \right)^2 \left(A_+^* \mathbf{T}_k \cdot \mathbf{T}_{ij} A_- \right)_{[\text{HELAS}]} \right), \quad (3.23)$$

where the CLBS is also taken in the helicity basis for the gluon emitter as in HELAS. The quantity $E_+ = \epsilon_{[\text{xz}c]}^+ \cdot L$ in Eq. (3.23) can be computed according to Eq. (3.19) in the conventions of [37] in terms of spinor products as (see e.g. [38])

$$e^{+i\phi(k)} E_+ = e^{+i\phi(\tilde{p}_{ij})} \frac{z_i \langle p_j p_i \rangle \langle \tilde{p}_{ij} p_i \rangle^*}{\sqrt{2} \langle p_j \tilde{p}_{ij} \rangle}, \quad (3.24)$$

where we have set $k = \tilde{p}_{ij}$ and chosen $q = p_j$ for the reference momentum in Eq. (3.21). Explicit expressions for the vector E_+ in Eq. (3.19) for all required momentum configurations (massless and massive) are given in Appendix B. For the dipole terms including the massive partons, the result for E_+ in Eq. (3.19) contains terms like $\langle p_i - |p_k| \tilde{p}_{ai} - \rangle$ with on-shell momenta $p_k^2 = m_k^2$. In order to express these terms through spinor products we have used flat momenta,

$$p_k^b = p_k - \frac{m_k^2}{2p_k \cdot \tilde{p}_{ai1}} \tilde{p}_{ai}, \quad (3.25)$$

which are massless because $(p_k^b)^2 = 0$. Due to the equations of motion $\not{p}_{ai} |\tilde{p}_{ai} - \rangle = 0$, we can rewrite the quantities under consideration, e.g.

$$\langle p_i - | \not{p}_k |\tilde{p}_{ai} - \rangle = \langle p_i - | \not{p}_k^b |\tilde{p}_{ai} - \rangle, \quad (3.26)$$

so that they are accessible to standard spinor calculus, see also [39] for the spinor helicity formalism including massive fermions. Our treatment of the spin correlations is contained in the Mathematica sources where the expressions for E_+ (as given in Appendix B) are implemented. During the automated generation of all subtraction terms for numerical evaluation the results are written to the output in the Fortran file, `dipole.f`, see Fig. 2.

3.5 Checking the soft and collinear limits

Let us discuss the checks for the AutoDipole package. First, there is the standard quality check on the automatic generation of the dipole terms because the result according to Eq. (2.3) has to be finite when approaching the singular regions. Second, since the Catani-Seymour formalism is well established, we can compare the output of AutoDipole with results of independent implementations in the literature.

The AutoDipole package performs automatically for all generated subtraction terms a numerical check of all IR limits. For that purpose the subtracted squared matrix element for the process under consideration are constructed and sampled over all limits to test the cancellation of the IR singularity. For a given soft/collinear limit L_i , we pick up the set $S(i)$ of the corresponding dipoles to test whether the quantity

$$\lim_{L_i} \left[|\mathcal{M}|^2 - \sum_{j \in S(i)} D(j) \right], \quad (3.27)$$

is soft/collinear safe. The code lists all limits L_i , and the corresponding sets $S(i)$. A concrete example will be presented in Subsection 4.2. The leading soft/collinear singularity of the squared matrix element $|\mathcal{M}|^2$ behaves in the soft limit as $1/k^2$ for a gluon of momentum k and in the collinear

one as $1/(2p_i \cdot p_j) = 1/s_{ij}$ for two collinear momenta p_i and p_j . The set of the corresponding dipoles cancels this leading singularity pointwise as

$$|\mathbf{M}|^2 - \sum_{j \in \mathcal{S}(i)} \mathbf{D}(j) = \frac{1}{x^2}(a_0 + a_1x + a_2x^2 + \dots) - \frac{1}{x^2}a_0, \quad (3.28)$$

where $x = k(\sqrt{s_{ij}})$ is the respective Lorentz scalar depending on the momenta in the soft (collinear) limit. The difference in Eq. (3.28) is integrable over the real emission phase space. The numerical accuracy, however, has to be controlled, because deep in the singular regions the individual contributions in Eq. (3.28) become very large and with the limited numerical precision of floating point arithmetic the cancellation might be imperfect. Fortunately, the stability of the numerical cancellation can be tested automatically. Normalizing Eq. (3.28) one can check the slope of the quantity,

$$\frac{|\mathbf{M}|^2 - \sum \mathbf{D}}{|\mathbf{M}|^2} = \frac{1}{a_0}(a_1x + a_2x^2 + \dots). \quad (3.29)$$

Based on Eq. (3.29) AutoDipole tests the cancellation and returns values for the fiducial regions for the Lorentz invariants s_{ij} .

We have extensively tested the soft and collinear finiteness of the generated subtraction terms for numerous scattering processes in e^+e^- , ep and pp -collisions including massive quarks and weak gauge bosons. Among those are a large class of $2 \rightarrow 4$ scattering processes as needed in the NLO QCD correction to $2 \rightarrow 3$ reactions. We have also tested scattering processes with $2 \rightarrow 5$ and $2 \rightarrow 6$ partons, like e.g.

$$\begin{aligned} u\bar{u} &\rightarrow d\bar{d}ggg \\ gg &\rightarrow W^+\bar{u}dgg \\ gg &\rightarrow t\bar{t}ggg \\ gg &\rightarrow t\bar{t}b\bar{b}g \\ gg &\rightarrow t\bar{t}b\bar{b}gg \end{aligned}$$

which are currently under investigation in view of phenomenological applications for the LHC. In addition, we have been able to obtain also perfect agreement with published results [36,40]. For the NLO QCD corrections to $pp \rightarrow t\bar{t} + 1\text{jet}$ production results for the real emission contributions have been presented at individual phase space points in [36]. We agree at least to 14 digits for the matrix elements squared and at least to 12 digits for the sum of the subtraction terms. All details of our comparison are shown in Table 5 in Appendix C. We have also checked against the results for the NLO QCD corrections to $pp \rightarrow W^+W^- + 1\text{jet}$ [40], in particular the real emissions in the channel $u\bar{u} \rightarrow W^+W^-gg$. Also here we have obtained very good agreement as documented in the last entry of Table 5. The AutoDipole package provides a shell script to reproduce some of the numbers in that Table 5 (see Section 4.4).

Let us briefly comment on the integrated dipoles in Eq. (2.3) originating from the \mathbf{I} -operators. Here, a complete check is more involved because for a given process scheme dependence enters, i.e. whether the singularities of the NLO virtual contributions are factorized with respect to the d -dimensional or 4-dimensional Born amplitude.

Nevertheless, partial checks of the singularity structure are straightforward. The matrix element squared with the sum of all \mathbf{I} -insertions is written schematically as

$$\langle 1, \dots, n | \mathbf{I} | 1, \dots, n \rangle = C_{-2} \frac{1}{\epsilon^2} + C_{-1} \frac{1}{\epsilon} + C_0, \quad (3.30)$$

where C_{-1} and C_{-2} are process (and kinematics) dependent coefficients. For the leading pole $\sim 1/\epsilon^2$, the coefficient C_{-2} obeys the following simple relation

$$C_{-2} = \frac{\alpha_s}{2\pi} |\mathbf{M}_{\text{Born}}|^2 \left((n_q + n_{\bar{q}}) C_F + n_g C_A \right), \quad (3.31)$$

where \mathbf{M}_{Born} is the corresponding Born amplitude. The number of external massless (anti-)quarks is n_q ($n_{\bar{q}}$) and n_g the number of external gluons. In QCD the standard $SU(N)$ color factors take the numerical values $C_F = 4/3$ and $C_A = 3$.

Apart from simple relations like Eq. (3.31) the coefficients for color and spin averaged results for the \mathbf{I} -operator could again be compared with the published literature for $pp \rightarrow t\bar{t} + 1\text{jet}$ production at NLO in QCD [36]. We have obtained agreement to at least 14 digits as shown in Table 6. The numbers in Table 6 can again be reproduced with a simple command explained in Section 4.4.

4 Running AutoDipole

This Section is meant to be a short manual to the AutoDipole package. We explain the installation procedure, the use and discuss a few processes as examples.

4.1 Install

The package, `AutoDipole_V1.2.3.tar`, is available for download from [41] (or else from the authors upon the request). In addition, one must also obtain the stand-alone version of MadGraph (`MG_ME_SA_V4.4.30`) e.g. by download from [42] and put it (in the form of `.tar.gz` or `.tar`) in the AutoDipole package directory. Then execute the installation procedure by¹

```
./install.sh
```

and the directory structure as displayed in Figure 1 emerges. Repetition of this command always allows the user to recover the initial settings described in this Section.

4.2 A short example

Let us next illustrate the use of AutoDipole. First of all, one has to specify all partonic real emission processes which appear at NLO in the observable under consideration. To that end, as a concrete example let us choose a simple process, $u\bar{u} \rightarrow d\bar{d}g$ which contributes to hadronic di-jet production,

¹ The AutoDipole package (version 1.2.3 and earlier) is assumed to be used with MadGraph (stand-alone version `MG_ME_SA_V4.4.30`). Upgrades to newer versions of MadGraph require the user to set the MadGraph version in the first line of `install.sh` by hand before installation. We have tested that AutoDipole version 1.2.3 also works with the MadGraph stand-alone version `MG_ME_SA_V4.4.39`. An automated test of the installation can be executed with the command `check.sh` as detailed in Section 4.4.

$pp \rightarrow 2$ jets at NLO. This example exhibits all features of the Catani-Seymour formalism, i.e. it needs dipoles and **I**-operators as well as the **P**- and **K**-terms. We start with the Mathematica part of AutoDipole. The package can simply be included through the driver file as

```
<<driver_user.m
```

Next, we can run the package for the process $u\bar{u} \rightarrow d\bar{d}g$ with the command

```
GenerateAll[{u,ubar},{d,dbar,g}]
```

Upon running the AutoDipole package successfully, all generated Fortran files are stored in a (newly created) directory under `process`, for the example at hand `./process/Proc_uux_ddxg`. AutoDipole returns the message:

```
*****'
Run has been succeeded.
In order to run the generated code, please enter
in the newly created directory under ./process
make
./runD
*****'
```

The real matrix element squared $|M|^2$ and the sum of all dipole terms $\sum_i D(i)$ are evaluated at 10 phase space points with this command. Also the check of cancellations in all infrared limits for the subtracted matrix element can be performed. The respective command is:

```
make checkIR
./checkIR
```

Likewise, the integrated dipoles (**I**-operators) as well as the contribution of the **P**- and **K**-terms at 10 points in phase space can be evaluated in the subdirectories `Proc_uux_ddxg/Virtual` and `Proc_uux_ddxg/PK` with the commands:

```
make runI
./runI
make runPK
./runPK.
```

The present example $u\bar{u} \rightarrow d\bar{d}g$ runs with the default settings of AutoDipole. For further illustration the package also comes along with a prepared list of examples so that explicit numbers can be obtained by executing the shell scripts explained in the next subsection.

If the user wants to include the generated Fortran code with the subtraction terms into his/her own project for further numerical evaluations, he/she needs (i.e. has to copy) a number of files for that purpose. The complete list of generated files is given in Table 1. Note that most of the functions are only needed internally and are not meant to be called by the user directly. We assume here that all input momenta $\{p_i\}$ are generated from phase space routines supplied by the user and that the HELAS library `libdheLas3.a` is linked.

Dipole terms : directory `process/Proc_uux_ddxg`

From the file `check.f` the call of the relevant subroutines for the evaluation of the dipole terms is obvious. The user needs to copy the following files:

file (subroutine)	input	output
<p>[Dipole terms]</p> <p>matrix.f (smatrix)</p> <p>dipole.f (dipole)</p> <p>reducedm.f (reducedm)</p> <p>cmatrix.f (cmatrix#)</p> <p>cmatrix.f (cmatrix#dh)</p> <p>check.f (program checkdipole)</p>	<p>$\{p_i\}$</p> <p>$\{p_i\}$</p> <p>$\{p_i\}$</p> <p>reduced $\{\tilde{p}_i\}$</p> <p>reduced $\{\tilde{p}_i\}$</p> <p>$\{p_i\}$ in inputm.h</p>	<p>$M ^2$ for real emission</p> <p>$D(i)$</p> <p>reduced $\{\tilde{p}_i\}$</p> <p>CLBS (like helicity)</p> <p>CLBS (unlike helicity)</p> <p>check of $D(i)$, $M ^2$</p>
<p>[I-terms]</p> <p>matrixL01.f (smatrix)</p> <p>Iterm.f (Iterm)</p> <p>cmatrix.f (cmatrix#)</p> <p>checkVirt.f (program checkVirt)</p>	<p>$\{p_i\}$</p> <p>$\{p_i\}$</p> <p>$\{p_i\}$</p> <p>$\{p_i\}$ in inputmLO.h</p>	<p>$M_{\text{Born}} ^2$</p> <p>C_i of I-terms</p> <p>CLBS</p> <p>check of C_i of I-terms</p>
<p>[P- and K-terms]</p> <p>matrixL01.f (smatrix)</p> <p>PKterm.f (PKterm)</p> <p>cmatrix.f (cmatrix#)</p> <p>checkPK.f (program checkPK)</p>	<p>$\{p_i\}$</p> <p>$\{p_i\}$</p> <p>$\{p_i\}$</p> <p>$\{p_i\}$ in inputmLO.h</p>	<p>$M_{\text{Born}} ^2$</p> <p>$Pt(i)$, $K(i)$ (P- and K-terms)</p> <p>CLBS</p> <p>check of $Pt(i)$ and $K(i)$</p>
<p>[Check of soft/collinear limits]</p> <p>collinear.f</p> <p>checkIR.f (program checkIR)</p>	<p>$\{p_i\}$</p> <p>collinear limit of $\{p_i\}$</p>	<p>collinear limits of $\{p_i\}$</p> <p>$(M ^2 - \sum D)/ M ^2$</p>
common input files		
<p>[Process dependent]</p> <p>allcolormat#.inc</p> <p>emitspecinfo.inc</p> <p>param_card.dat</p> <p>nexternal.inc</p> <p>nexternal2.inc</p> <p>inputm.h</p> <p>inputmLO.h</p> <p>[Process independent]</p> <p>coupl.inc</p> <p>couplings.f</p>	<p>extended color matrices (used in cmatrix#)</p> <p>information of emitter for dipoles (used in cmatrix#)</p> <p>parameters for CLBS</p> <p>field numbers of real emission process for dipoles and of Born process for I-, P- and K-terms</p> <p>field number of reduced Born process</p> <p>phase space points for dipole checks</p> <p>phase space points for I-, P-, and K-term checks</p> <p>common block of parameters</p> <p>reads parameters in param_card.dat and assigns them in coupl.inc</p>	

Table 1: The file content of the AutoDipole package. In names of subroutine and files (e.g. cmatrix#) the symbol # denotes an integer number, typically #=1.

matrix.f	(generated by AutoDipole)
dipole.f	
reducedm.f	
cmatrix.f	
allcolormat\#.inc	
emitspecinfo.inc	
nexternal.inc	
nexternal2.inc	(generated by AutoDipole)
coupl.inc	(process independent file)
couplings.f	(process independent file)
param_card.dat	(parameter input file)

To use the generated code, one first has to initialize MadGraph. The parameters are determined in `param_card.dat` and are assigned to the definitions in `coupl.inc` with the help of the subroutine `setpara` in `couplings.f` as

```
include 'coupl.inc'
call setpara('param_card.dat',.true.)
```

to be used subsequently in the subroutines `cmatrix#`, `cmatrix#dh`, and `smatrix` through the common blocks. The symbol `#` here and above denotes an integer number (e.g. `#=1`). For the dipoles only the strong coupling constant α_s as well as the top and bottom masses are needed in the evaluation. These three parameters appear as

```
AL=g**2*(4.d0*pi)**(-1)
mt=tmass
mb=bmass
```

and are passed to the subroutine `dipole` through the common blocks,

```
common /usedalpha/ AL
common /MASS/ mt,mb
```

Next, the evaluation of the squared matrix element for the real emission process $|M|^2$ proceeds in exactly the same way as in MadGraph with the call

```
call smatrix(p,msq)
```

Finally, the dipole terms are evaluated by calling the subroutine

```
call dipole(p,dip,SumD)
```

which returns an array with the values for each dipole term (`dip`) and the sum of the all dipoles (`SumD`) as output. For our example process $u\bar{u} \rightarrow d\bar{d}g$ we have 15 individual dipoles. The reduced kinematics of each dipole (as determined by the subroutine `reducedm`) can be accessed by the common block

```
double precision ptil(0:3,1:n1,n2)
common /OUTPUTM/ ptil
```

where $n1=4$ and $n2=15$ in the definition of the momenta for the example at hand.

I-terms : directory `process/Proc_uux_ddxg/Virtual`

Our program `checkVirt.f` for checks of the **I**-terms again provides an example for the use of the subroutines to evaluate the **I**-terms. In addition to the eight files from `cmatrix.f` to `param_card.dat` listed above for the evaluation of the dipoles, the user has to copy one file:

`Iterm.f`

Then, the initialization phase is exactly the same as before and for the evaluation of the **I**-terms, one has to call the subroutine

```
call Iterm(p,coef,SumI)
```

which provides the value of the coefficients (i.e. the array `coef`) as well as the sum (`SumI`) of all **I**-terms as output. If the user also wants to compute the LO matrix element $|M_{\text{Born}}|^2$ he needs the file `matrixL01.f`. The execution of the subroutine with the command

```
call smatrix(p,msqL0)
```

is performed again exactly as in `MadGraph`.

P- and K-terms : directory `process/Proc_uux_ddxg/PK`

The user needs the following file to evaluate the **P**- and **K**-terms:

```
PKterm.f
matrixL01.f
```

as well as the eight files from `cmatrix.f` to `param_card.dat` already discussed for the dipoles. The initialization phase is unchanged but the user has to provide the parton momentum fraction x from the mass factorization as additional input. The **P**- and **K**-terms for the first leg are computed by the call

```
call PKterm1(p,x,SumP,SumK)
```

which returns separately the sum of all **P**- and **K**-terms (`SumP` and `SumK`). For the second parton in initial state (as in hadron-hadron collisions) the corresponding **P**- and **K**-terms are evaluated by calling `PKterm2`.

4.3 General usage

For a specific application of `AutoDipole`, the user needs to perform the following three steps:

1. Setup of parameters : `parameter.m`
2. Run of package : `GenerateAll[{initial},{final}]`
3. Run and checks of the generated code at : `/process/Proc_xx_xx/` .

Let us explain each of these steps in more detail.

1. Setup of parameters

Generally, the user has to supply all process parameters needed for the dipole subtraction procedure by editing the file,

`parameter.m`

where (following the MadGraph conventions) all values with the dimension of a mass are in units of [GeV]. Let us explain all variables in the file together with the chosen default values.

Parameters for dipole terms

`ep=0` :

The parameter of dimensional regularization of space-time, $D = 4 - 2\epsilon$. The default choice eliminates higher orders (positive powers) of ϵ in the dipole terms.

`kap=2/3` :

κ is free parameter in some expressions for massive dipoles [2]. The value $\kappa = 0$ leads to the simplest results for the dipole terms, while $\kappa = 2/3$ produces the simplest expressions of the **I**-terms.

`skipdipole={ }` :

This set specifies the kind of dipoles to be skipped during the creation. For example, the set `skipdipole={2t}` omits the creation of the Dipole 2-(5) with the $t - \bar{t}$ splitting (see Table 2 in Appendix A).

`mur=174.30` :

The value of the renormalization scale. The default value is the same as the default value of the top-quark mass in MadGraph.

`accut=10-3` :

This value is used for the checking the quality of the infrared cancellations in the generated code upon scanning over all possible collinear configurations.

Parameters for **I**-terms

`mFlist={ }` :

This set lists all heavy quarks which possibly contribute to the **I**-terms with a gluon emitter in final state, e.g. as `mFlist={t,b}`.

`lightflavors=1` :

This is the number of the light flavors which contributes to the **I**-terms with a gluon emitter in initial and final states.

`replistVirtual={ }` :

This set enables user defined symbolic replacements to simplify the virtual contribution, e.g. of the type, `replistVirtual={Gamma[1-eps]-> (4*Pi)eps*somesymbol-1}` which results in the replacement, $\frac{(4\pi)^\epsilon}{\Gamma(1-\epsilon)} = \text{somesymbol}$.

`sjexpansion=0` :

This parameter determines whether the typical factors of dimensional regularization like $\left(\frac{4\pi\mu^2}{2p_i \cdot p_j}\right)^\epsilon$ in the **I**-terms are expanded (0) or not (1).

Parameters for **P**- and **K**-terms

`KFSff=0`, `KFSgg=0`, `KFSfg=0`, and `KFSgf=0` :

These parameters specify the factorization scheme. In the $\overline{\text{MS}}$ scheme (default choice) they are all vanishing.

`lightquarksPK3={u}` :

This set specifies all light flavors to be added to the initial gluon of the reduced Born process in the **P**- and **K**-terms (see group (6) in Table 4 in Appendix A).

`muFfort=174.30` :

This is the value of the factorization scale μ_F , which has the same default value as the renormalization scale μ_R .

The other parameters which are used by MadGraph are determined in the file `patch/Models/sm/param_card.dat`.

The default values for the most important ones are the following (in units of [GeV] for masses),

`$\alpha_s=0.1180$`

`$\alpha_{em}=0.007547169811320755$`

`Top mass=174.3`

`Bottom mass=4.7`

`W mass=80.419`

`Z mass=91.188`

`Higgs mass=120.0`

These parameters are used consistently throughout the run of the package. Any other changes of SM parameters like e.g. G_F , the CKM-parameters, the decay widths of heavy fields, and so on, are done in the same MadGraph file, `param_card.dat`. Similarly, also control over all interactions in the SM proceeds entirely through MadGraph, i.e. through the file,

`patch/Models/sm/interactions.dat`

in the exactly same way as in the normal use of MadGraph. All MadGraph parameters are explained in [42].

2. Run of package

For general QCD processes (including leptons and SM bosons) we run AutoDipole by executing the Mathematica command:

```
GenerateAll[{initial},{final}]
```

where the sets labeled `initial` and `final` contain all external particles of the respective scattering process. The following fields are available in the present version of the package:

Fermions:

$$(u, d, b, t, e^-, \mu^-, \bar{u}, \bar{d}, \bar{b}, \bar{t}, e^+, \mu^+) = (u, d, b, t, e, \text{muon}, \text{ubar}, \text{dbar}, \text{bbar}, \text{tbar}, \text{ebar}, \text{muonbar}) ,$$

Bosons:

$$(gluon, photon, W^+, W^-, Z, Higgs) = (g, \text{gamma}, Wp, Wm, Z, h) ,$$

where the right hand side denotes the input format of AutoDipole. The available quark fields include the first family (u and d -quarks) which serves as a template for light quarks and, respectively, the third family (b and t -quarks) as one for heavy quarks. In practice this suffices as far as the subtraction formalism is concerned, because generally QCD scattering processes at NLO will be insensitive to the individual flavor of the quarks, and the sum over all light quark flavors can be trivially taken afterwards. If one intends to study particular channels, e.g. in W^\pm production, flavor separation is required, though.

As a result of the run, AutoDipole produces the following information about the created dipoles and the **I**-, **P**- and **K**-terms:

- All analytical expressions for the dipole terms are written in the order given in Table 2 along with the reduced Born process (emitter,spectator) and the reduced kinematics for each dipole term. Also, the number of created dipole terms is shown group by group, namely Dipole 1, 2, 3, and 4 and their subgroups (see Figure 3). The number of massive dipole terms is given separately.
- All soft and collinear limits together with the corresponding dipole terms are returned. For example, for the process $g(1)g(2) \rightarrow t(3)\bar{t}(4)g(5)g(6)$ (see next Subsection) the fifth collinear limit is denoted $Lc(5) = (5, 6) : Sc(5) = \{17, 18, 19, 20\}$. This means that the collinear divergence of the pair $(5(g), 6(g))$ is canceled by the set of the dipoles, $Sc(5)$ and the set consists of the dipoles number 17, 18, 19, and 20. In the same way, the soft limit and the corresponding dipoles are displayed. E.g. for the soft limit of gluon 5(g), $Ls(1) = (5) : Ss(1) = \{Sc(1), Sc(2), Sc(5), Sc(6), Sc(7)\}$, which means that the soft divergence of 5(g) is canceled by the set of the dipoles, $Ss(1)$. This set in turn consists of the sets of collinear limits $Sc(1)$, $Sc(2)$, and so on.
- The analytical expressions of all **I**-terms are shown in the order as given in Table 3 prior to the expansion in ϵ as well as the individual coefficients of the poles C_{-2} , C_{-1} , and C_0 (see Eq. (3.30)) after the ϵ expansion. Also the total number of all created **I**-terms is displayed by group by group (see Table 3).
- The analytical expressions of all created **P**- and **K**-terms are shown in the order given in Table 4 together with the total number of **P**- and **K**-terms.
- Finally, AutoDipole outputs a summary with the numbers of all created dipoles, **I**-, **P**- and **K**-terms and the reduced Born processes.

This information, being rather detailed, helps with the identification of individual terms according to the order of creation. The Mathematica part of AutoDipole provides analytical and symbolic expressions, which are easily accessible, if needed. These features are primarily for an experienced user.

Upon running the AutoDipole package it occurs (on purely algorithmic grounds) in some cases though, that a particular reduced Born cross section does not exist. For example, the process $e^-e^+ \rightarrow u\bar{u}g$ does give rise through the dipole 2-(5)-(u, \bar{u}) to the Born process $e^-e^+ \rightarrow gg$, which does not exist at tree level. In such cases, an error message is displayed:

```
Reduced Born amplitude B2u does not exist.
Dipole 2u must be switched off.
Please set in the file ./parameter.m
skipdipole={ 2u }
```

Following the message the user has to modify the command `skipdipole` and repeat the Mathematica run. In this way only the relevant partial subsets of dipole terms is extracted and the offending Born processes are skipped (thanks to `skipdipole`) before calling the MadGraph part.

3. Run and checks of the generated code

Finally, as briefly explained above, the user can run the generated Fortran code for the regularized real emission process as well as the **I**-, **P**- and **K**-terms. The checks proceed as follows:

Dipole terms

As mentioned above, the evaluation of the real matrix element squared $|M|^2$ and the sum of all dipole terms $\sum_i D(i)$ at 10 randomly chosen phase space points as well as the check of cancellations in all infrared limits for the subtracted matrix element are automatically executed:

```
make
./runD
```

```
make checkIR
./checkIR
```

The latter command performs a scan over all possible collinear configurations. For the expression

$$\frac{|M|^2 - \sum D}{|M|^2}, \quad (4.1)$$

cf. Eq. (3.29), it is checked whether the cancellation works at least to the accuracy defined by the value of the parameter `accut` in the file `parameter.m`. If the absolute value of the normalized subtracted squared matrix element in Eq. (3.29) drops below the pre-defined value of `accut` sufficiently deep in the collinear limit, the message,

```
Infrared safety of all collinear limits is confirmed for S_ij/S > ...
```

is printed.

I-terms

The Fortran code to evaluate all **I**-terms is collected in the subdirectory `./Virtual`. There, the coefficients of the double and single poles in the ϵ expansion C_{-2} , C_{-1} , C_0 in Eq. (3.30) can be evaluated at 10 randomly chosen phase space points by:

```
make runI
./runI
```

This includes in particular the calculation of the double poles according to

$$\frac{C_{-2}}{(\alpha_s/2\pi)|M_{\text{Born}}|^2}, \quad (4.2)$$

and the user can easily confirm that Eq. (3.31) holds.

P- and K-terms

Likewise, the mass factorization terms originating from the **P** and **K**-terms is stored in `./PK` and also evaluated at 10 randomly chosen phase space points by the command:

```
make runPK
./runPK
```

This concludes our brief description of the user specific features of the AutoDipole package.

4.4 Examples

The package includes a command to demonstrate the run for several example processes. This helps to explain the package and at the same time confirms that the installation was done successfully and that the package works properly. These examples include the computation of some of the numbers given in Tables 5 and 6 in Appendix C. The command

```
./lib/sh/check.sh
```

generates five processes in different kinematics,

1. $e^-e^+ \rightarrow u\bar{u}g$
2. $e^-u \rightarrow e^-ug$
3. $gg \rightarrow t\bar{t}gg$
4. $ug \rightarrow t\bar{t}ug$
5. $u\bar{u} \rightarrow W^+W^-gg$

provides suitable settings for the parameters of each process and runs the package. For illustration, we only explain in the following those settings which are changed with respect to the default ones. The processes from 1 to 4 use a value of $\alpha_s=0.1075205492734706$ from [36] for the strong coupling constant. For the processes 1 and 2 the contribution of the Z -boson exchange is switched off in the file `interactions.dat` for simplicity. Moreover, in `parameter.m` the splitting $2u$ in process 1 (and $3u$ in 2) is skipped by the command `skipdipole = {2u}` (and `skipdipole = {3u}` in 2, respectively) to exclude an inexistent reduced Born process.

For the processes 3 and 4 the QED interaction is switched off in the file `interactions.dat` in order to focus on the QCD corrections only. Furthermore, a value of 174 [GeV] for the top mass is used following [36] and the decay width of the top-quark must be switched off in the file `param_card.dat`. For the comparison with [36] the $t-\bar{t}$ splitting is skipped in `parameter.m`,

i.e. `skipdipole = {2t}`, and the renormalization and factorization scales are set equal to the top mass value. For the **I**-terms five light flavors are taken into account, `lightflavors = 5`.

Finally, process 5 uses the following settings [40] in the file `param_card.dat`: W -mass=80.425, $\alpha_s = 0.1202629003906369$, $\alpha_{em} = 0.007543595708669335$ and Fermi's constant $G_F = 1.16637 \times 10^{-5}$, and the decay width of W -boson is switched off. The results of processes 3, 4, and 5 should reproduce the corresponding numbers in Tables 5 and 6.

The test run of all examples is finally checked by comparing all computed values of the dipoles, **I**-terms, and the averaged matrix element squared $|M|^2$ for the processes 1 to 5 the with ones in the data files in `./lib/check/`. At the end of the run, e.g. for example 3, the following message appears:

```
3.gg_ttxgg
  |M|^2(Real) :Confirmed
  Dipole      :Confirmed
  |M|^2(LO)   :Confirmed
  I-term      :Confirmed
```

This confirms the successful installation and proper functioning of the package. The generated code for all examples is stored in the directory `./process` as in a usual run and the directory of each process includes in the file `res_std` the result of the comparison with the data files from `./lib/check/`. All parameters used for each process are accessible in `param_card.dat`, so the user can also run the respective files individually with usual commands of the previous subsection.

5 Conclusion

We have presented the package `AutoDipole` which provides an implementation of the Catani-Seymour dipole formalism [1, 2] to compute subtracted matrix elements squared in an automatic way. The package (partial aspects of which have been discussed before [17, 18]) consists of essentially three ingredients: the automatic generation of all dipole terms via `Mathematica` routines as well as the calculation of the color-correlated matrix elements and the evaluation of different helicity amplitudes with the help of `MadGraph` [3–5] (i.e. a patched stand-alone version).

We have presented a complete discussion of the set-up of the program and the details of our implementation as well as the numerical evaluation of the squared matrix elements. Particular emphasis has been put on explaining the use of `AutoDipole` which has been illustrated with sufficiently non-trivial examples. The finiteness in the soft and collinear limits has been demonstrated for a large number of processes in e^+e^- , ep and pp -scattering. Also, checks for the complete set of dipoles have been performed by comparing to various processes in the recent literature.

In comparison with other available software to generate subtraction terms for the real emission contributions `AutoDipole` has a number of advantages. First of all, the algorithm is implemented in a way so that analytic expressions are generated which are accessible to symbolic manipulation. Then, the chosen order for the dipole generation produces flat Fortran code and allows to handle scattering processes with $2 \rightarrow 5$ and $2 \rightarrow 6$ partons of relevance for LHC phenomenology including the computation of the CLBS. Finally, the structure of the package is highly modular and flexible for further extensions.

Future improvements of the AutoDipole package will address restricting the dipoles to small regions of phase space, as realized e.g. through α -parameters [43]. This is advantageous when performing the Monte Carlo integration over the phase space of the real emission process. The implementation of such cuts affects also the integrated dipoles and the case of massless partons is available in the literature whereas for the case of massive partons most cases can be found in [44, 45]. The remaining integrals for exhaustive coverage can be done e.g. with the methods of [32]. Next, the current version of AutoDipole does not cover processes with identified hadrons in the final state where one needs fragmentation. Here, the so-called **H**-terms have to be taken into account, which will be implemented in a later version of AutoDipole. Finally, the structure of our code is particularly suited for extensions to physics beyond the Standard Model (BSM). The main modification needed is the so-called model file of MadGraph, which is currently already available for a large class of BSM scenarios including e.g. the minimal supersymmetric extension of Standard Model for which the necessary modifications of the dipole formalism are known [2]. All the extensions mentioned above can be easily realized within the existing structure of our code.

The AutoDipole package is available for download from [41] or from the authors upon request. The MadGraph package (stand-alone version) which includes the HELAS library may be obtained from [42].

Acknowledgments

We acknowledge useful discussions with S. Badger, T. Diakonidis, R. Frederix, F. Maltoni, T. Riemann, and B. Tausk. This work is supported in part by the Deutsche Forschungsgemeinschaft in Sonderforschungsbereich/Transregio 9, the European Community in Marie-Curie Research Training Network MRTN-CT-2006-035505 “*HEPTOOLS*”, and the Helmholtz Gemeinschaft under contract VH-NG-105 and contract VH-HA-101 (Alliance “*Physics at the Terascale*”).

References

- [1] S. Catani and M.H. Seymour, Nucl. Phys. B485 (1997) 291, hep-ph/9605323.
- [2] S. Catani et al., Nucl. Phys. B627 (2002) 189, hep-ph/0201036.
- [3] T. Stelzer and W.F. Long, Comput. Phys. Commun. 81 (1994) 357, hep-ph/9401258.
- [4] F. Maltoni and T. Stelzer, JHEP 02 (2003) 027, hep-ph/0208156.
- [5] J. Alwall et al., JHEP 09 (2007) 028, arXiv:0706.2334 [hep-ph].
- [6] K. Hagiwara, H. Murayama and I. Watanabe, Nucl. Phys. B367 (1991) 257.
- [7] H. Murayama, I. Watanabe and K. Hagiwara, KEK-91-11.
- [8] F. Bloch and A. Nordsieck, Phys. Rev. 52 (1937) 54.
- [9] T. Kinoshita, J. Math. Phys. 3 (1962) 650.
- [10] T.D. Lee and M. Nauenberg, Phys. Rev. 133 (1964) B1549.
- [11] W.T. Giele and E.W.N. Glover, Phys. Rev. D46 (1992) 1980.
- [12] W.T. Giele, E.W.N. Glover and D.A. Kosower, Nucl. Phys. B403 (1993) 633, hep-ph/9302225.
- [13] S. Keller and E. Laenen, Phys. Rev. D59 (1999) 114004, hep-ph/9812415.
- [14] B.W. Harris and J.F. Owens, Phys. Rev. D65 (2002) 094032, hep-ph/0102128.

- [15] S. Frixione, Z. Kunszt and A. Signer, Nucl. Phys. B467 (1996) 399, hep-ph/9512328.
- [16] L. Phaf and S. Weinzierl, JHEP 04 (2001) 006, hep-ph/0102207.
- [17] K. Hasegawa, S. Moch and P. Uwer, Nucl. Phys. Proc. Suppl. 183 (2008) 268, arXiv:0807.3701 [hep-ph].
- [18] K. Hasegawa, S. Moch and P. Uwer, Nucl. Phys. Proc. Suppl. 186 (2009) 86.
- [19] T. Gleisberg and F. Krauss, Eur. Phys. J. C53 (2008) 501, arXiv:0709.2881 [hep-ph].
- [20] M.H. Seymour and C. Tevlin, (2008), arXiv:0803.2231 [hep-ph].
- [21] R. Frederix, T. Gehrmann and N. Greiner, JHEP 09 (2008) 122, arXiv:0808.2128 [hep-ph].
- [22] M. Czakon, C.G. Papadopoulos and M. Worek, (2009), arXiv:0905.0883 [hep-ph].
- [23] R. Frederix et al., (2009), arXiv:0908.4272 [hep-ph].
- [24] A. Gehrmann-De Ridder, T. Gehrmann and E.W.N. Glover, Nucl. Phys. B691 (2004) 195, hep-ph/0403057.
- [25] S. Weinzierl, JHEP 03 (2003) 062, hep-ph/0302180.
- [26] S. Frixione and M. Grazzini, JHEP 06 (2005) 010, hep-ph/0411399.
- [27] G. Somogyi, Z. Trocsanyi and V. Del Duca, JHEP 06 (2005) 024, hep-ph/0502226.
- [28] A. Gehrmann-De Ridder, T. Gehrmann and E.W.N. Glover, JHEP 09 (2005) 056, hep-ph/0505111.
- [29] G. Somogyi and Z. Trocsanyi, JHEP 01 (2007) 052, hep-ph/0609043.
- [30] G. Somogyi, Z. Trocsanyi and V. Del Duca, JHEP 01 (2007) 070, hep-ph/0609042.
- [31] U. Aglietti et al., JHEP 09 (2008) 107, arXiv:0807.0514 [hep-ph].
- [32] P. Bolzoni et al., JHEP 08 (2009) 079, arXiv:0905.4390 [hep-ph].
- [33] A. Mitov and S. Moch, JHEP 05 (2007) 001, hep-ph/0612149.
- [34] E.G. Floratos, C. Kounnas and R. Lacaze, Nucl. Phys. B192 (1981) 417.
- [35] S. Dittmaier, P. Uwer and S. Weinzierl, Phys. Rev. Lett. 98 (2007) 262002, hep-ph/0703120.
- [36] S. Dittmaier, P. Uwer and S. Weinzierl, Eur. Phys. J. C59 (2009) 625, arXiv:0810.0452 [hep-ph].
- [37] Z. Xu, D.H. Zhang and L. Chang, Nucl. Phys. B291 (1987) 392.
- [38] S. Weinzierl, SACLAY-SPH-T-98-083.
- [39] C. Schwinn and S. Weinzierl, JHEP 05 (2005) 006, hep-th/0503015.
- [40] S. Dittmaier, S. Kallweit and P. Uwer, Phys. Rev. Lett. 100 (2008) 062003, arXiv:0710.1577 [hep-ph].
- [41] AutoDipole <http://www-zeuthen.desy.de/~moch/autodipole> or <http://www.physik.hu-berlin.de/pep/tools/>.
- [42] MadGraph <http://madgraph.hep.uiuc.edu/> or <http://madgraph.phys.ucl.ac.be/> or <http://madgraph.roma2.infn.it/>.
- [43] Z. Nagy and Z. Trocsanyi, Phys. Rev. D59 (1999) 014020, hep-ph/9806317.
- [44] J.M. Campbell, R.K. Ellis and F. Tramontano, Phys. Rev. D70 (2004) 094012, hep-ph/0408158.
- [45] J.M. Campbell and F. Tramontano, Nucl. Phys. B726 (2005) 109, hep-ph/0506289.

Appendix

A Creation order of subtraction terms

Emitter	Spectator	Dipole	Condition	Eq.
Dipole 1				
(1) $(i, j) = (f, g)$	1. k	$D_{ij,k}$	$m_i = m_k = 0$	(5.7) in [1]
		$DM_{ij,k}$	$m_i \neq 0$ or $m_k \neq 0$	(5.16) in [2]
	2. b	D_{ij}^b	$m_i = 0$	(5.39) in [1]
		DM_{ij}^b	$m_i \neq 0$	(5.50) in [2]
(2) $(i, j) = (g, g)$	3. k	$D_{ij,k}$	$m_k = 0$	(5.9) in [1]
		$DM_{ij,k}$	$m_k \neq 0$	(5.19) in [2]
	4. b	D_{ij}^b	---	(5.40) in [1]
(3) $(a, i) = (f, g)$	5. k	D_k^{ai}	$m_k = 0$	(5.65) in [1]
		DM_k^{ai}	$m_k \neq 0$	(5.81) in [2]
	6. b	$D^{ai,b}$	---	(5.145) in [1]
(4) $(a, i) = (g, g)$	7. k	D_k^{ai}	$m_k = 0$	(5.68) in [1]
		DM_k^{ai}	$m_k \neq 0$	(5.85) in [2]
	8. b	$D^{ai,b}$	---	(5.148) in [1]
Dipole 2				
(5) $(i, j) = (f, \bar{f})$				
$(i, j) = (u, \bar{u})$	9u. k	$D_{ij,k}$	$m_k = 0$	(5.8) in [1]
		$DM_{ij,k}$	$m_k \neq 0$	(5.17) in [2]
	10u. b	D_{ij}^b	---	(5.41) in [1]
$(i, j) = (t, \bar{t})$	9t. k	$DM_{ij,k}$	---	(5.17) in [2]
	10t. b	DM_{ij}^b	---	(5.51) in [2]
Dipole 3				
(6) $(a, i) = (f, f)$				
$(a, i) = (u, u)$	11u. k	D_k^{ai}	$m_k = 0$	(5.67) in [1]
		DM_k^{ai}	$m_k \neq 0$	(5.83) in [2]
	12u. b	$D^{ai,b}$	---	(5.147) in [1]
Dipole 4				
(7) $(a, i) = (g, f)$				
$(a, i) = (g, u)$	13u. k	D_k^{ai}	$m_k = 0$	(5.66) in [1]
		DM_k^{ai}	$m_k \neq 0$	(5.82) in [2]
	14u. b	$D^{ai,b}$	---	(5.146) in [1]

Table 2: The emitter pair is denoted (i, j) or (a, i) and, respectively, the spectator $k(\neq i, j)$ or $b(\neq a)$. D is a massless dipole and DM is a massive dipole. The equation numbers refer to [1] for massless dipoles (D) and to [2] for massive ones (DM). Dipole 2 has the other flavors, massless down and massive bottom quarks. Dipole 3 and 4 have also the other light flavors, $f = \bar{u}, d, \bar{d}$.

Emitter	Spectator	I-terms	Condition	Eq.
(1) $i = f$	1. k	$I_f(i, k)$	$m_i = m_k = 0$	(C.27) in [1]
		$IM1(i, k)$	$m_i \neq 0$ or $m_k \neq 0$	(6.16) in [2]
	2. b	$I_f(i, b)$	$m_i = 0$	(C.27) in [1]
		$IM2(i, b)$	$m_i \neq 0$	(6.52) in [2]
(2) $i = g$	3. k	$I_g(i, k)$	$m_k = \{m_F\} = 0$	(C.27) in [1]
		$IM3(i, k)$	$m_k \neq 0$ or $\{m_F\} \neq 0$	(6.16) in [2]
	4. b	$I_g(i, b)$	$\{m_F\} = 0$	(C.27) in [1]
		$IM4(i, b)$	$\{m_F\} \neq 0$	(6.52) in [2]
(3) $a = f$	5. k	$I_f(a, k)$	$m_k = 0$	(C.27) in [1]
		$IM5(a, k)$	$m_k \neq 0$	(6.52) in [2]
	6. b	$I_f(a, b)$	---	(C.27) in [1]
(4) $a = g$	7. k	$I_g(a, k)$	$m_k = 0$	(C.27) in [1]
		$IM7(a, k)$	$m_k \neq 0$	(6.52) in [2]
	8. b	$I_g(a, b)$	---	(C.27) in [1]

Table 3: The emitter is denoted i or a and, respectively, the spectator $k(\neq i)$ or $b(\neq a)$. I is the massless insertion operator and IM is a massive one. The equation numbers refer to [1] for massless insertions (I) and to [2] for massive ones (IM). The set of the heavy-quark masses the running in the quark loop are abbreviated $\{m_F\}$.

Emitter pair	Spectator	P and K	Condition	Eq.
Dipole 1				
(3) $(a, a', i) = (f, f, g)$		$K_0^{aa'}$	---	(C.17) in [1]
	5. k	$P_k^{aa'}$	---	(C.29) in [1]
		$K_k^{aa'}$	$m_k = 0$	(C.31) in [1]
		$KM_k^{aa'}$	$m_k \neq 0$ or $\{m_F\} \neq 0$	(6.55) in [2]
	6. b	$P^{aa',b}$	---	(C.29) in [1]
		$K^{aa',b}$	---	(C.33) in [1]
(4) $(a, a', i) = (g, g, g)$		$K_0^{aa'}$	---	(C.18) in [1]
	7. k	$P_k^{aa'}$	---	(C.29) in [1]
		$K_k^{aa'}$	$m_k = 0$	(C.31) in [1]
		$KM_k^{aa'}$	$m_k \neq 0$ or $\{m_F\} \neq 0$	(6.55) in [2]
	8. b	$P^{aa',b}$	---	(C.29) in [1]
		$K^{aa',b}$	---	(C.33) in [1]
Dipole 3				
(6) $(a, a', i) = (f, g, f)$				
$(a, a', i) = (u, g, u)$		$K_0^{aa'}$	---	(C.15) in [1]
	11 <u>. k</u>	$P_k^{aa'}$	---	(C.29) in [1]
		$KM_k^{aa'}$	$m_k \neq 0$	(6.55) in [2]
	12 <u>. b</u>	$P^{aa',b}$	---	(C.29) in [1]
		$K^{aa',b}$	---	(C.33) in [1]
Dipole 4				
(7) $(a, a', i) = (g, f, \bar{f})$				
$(a, a', i) = (g, u, \bar{u})$		$K_0^{aa'}$	---	(C.16) in [1]
	13 <u>. k</u>	$P_k^{aa'}$	---	(C.29) in [1]
		$KM_k^{aa'}$	$m_k \neq 0$	(6.55) in [2]
	14 <u>. b</u>	$P^{aa',b}$	---	(C.29) in [1]
		$K^{aa',b}$	---	(C.33) in [1]

Table 4: The emitter is denoted a' and different from spectator $b(\neq a')$. The massless case is abbreviated K and massive one KM. The equation numbers refer to [1] for massless insertions (K) and to [2] for massive ones (KM). For the cases Dipole 3 and 4, f can take the light flavors $f = u, \bar{u}, d, \bar{d}$ and so on.

B Correlation functions of gluon emitter

We use the following definitions of spinor products [37]:

$$\langle k_1 k_2 \rangle = \sqrt{k_1^- k_2^+} e^{+i\phi(k_1)} - \sqrt{k_1^+ k_2^-} e^{+i\phi(k_2)} \quad (\text{B.1})$$

$$k^\pm = |\vec{k}| \pm k_z \quad (\text{B.2})$$

$$e^{+i\phi(k)} = \frac{k_\perp}{|k_\perp|} \quad (\text{B.3})$$

$$k_\perp = k_x + ik_y \quad (\text{B.4})$$

If the reduced momentum of the initial gluon emitter lies in z-axis with $l = E_l(1, 0, 0, \pm 1)$ the spinor product are defined as $\langle p_i \tilde{p}_{ai} \rangle_z$ to avoid an ambiguity in the intermediate steps of the calculation,

$$\langle kl \rangle_z = \begin{cases} \sqrt{2E_l k^-} e^{+i\phi(k)} & (E_l = l_z) \\ -\sqrt{2E_l k^+} & (E_l = -l_z) \end{cases} \quad (\text{B.5})$$

$$\langle l_1 l_2 \rangle_z = \begin{cases} -2\sqrt{E_1 E_2} & (E_1 = l_{1z} \text{ and } E_2 = -l_{2z}) \\ 2\sqrt{E_1 E_2} & (E_1 = -l_{1z} \text{ and } E_2 = l_{2z}) \end{cases} \quad (\text{B.6})$$

The explicit forms of $e^{+i\phi(k)} E_+$ in Eq. (3.23) are shown for all massless and massive dipoles with a gluon emitter. Here we write the quantity including the phase difference as $E'_+ = e^{+i\phi(k)} E_+$. The reduced momenta are ones used in the corresponding equations in [1, 2], which are shown in Table 2. The \tilde{p}_{ij1} and \tilde{p}_{ai} are massless and the $p\tilde{M}_{ij}$ are massive ones.

Massless momenta

[Dipole 1-(2)-3($m_k = 0$) and Dipole 2-(5)-9u($m_k = 0$)]

$$E1'_+ = e^{+i\phi(\tilde{p}_{ij})} \frac{z_i \langle p_j p_i \rangle \langle \tilde{p}_{ij} p_i \rangle^*}{\sqrt{2} \langle p_j \tilde{p}_{ij} \rangle} \quad (\text{B.7})$$

[Dipole 1-(2)-4 and Dipole 2-(5)-10u($m_k = 0$)]

$$E2'_+ = e^{+i\phi(\tilde{p}_{ij})} \frac{z_i \langle p_j p_i \rangle \langle \tilde{p}_{ij} p_i \rangle^*}{\sqrt{2} \langle p_j \tilde{p}_{ij} \rangle} \quad (\text{B.8})$$

[Dipole 1-(4)-7($m_k = 0$) and Dipole 3-(6)-11u($m_k = 0$)]

$$E3'_+ = \frac{\langle p_i p_k \rangle \langle p_k \tilde{p}_{ai} \rangle_z^*}{\sqrt{2} (1 - u_i) \langle p_i \tilde{p}_{ai} \rangle_z} \quad (\text{B.9})$$

[Dipole 1-(4)-8 and Dipole 3-(6)-12u]

$$E4'_+ = \frac{-s_{ai} \langle p_i p_b \rangle_z \langle \tilde{p}_{ai} p_b \rangle_z}{\sqrt{2} s_{ab} \langle p_i \tilde{p}_{ai} \rangle_z} \quad (\text{B.10})$$

Massive momenta

[Dipole 1-(2)-3($m_k \neq 0$) and Dipole 2-(5)-9u($m_k \neq 0$)]

$$EM1'_+ = e^{+i\phi(p\tilde{M}_{ij})} \frac{z_i^{(m)} \langle p_j p_i \rangle \langle p\tilde{M}_{ij} p_i \rangle^*}{\sqrt{2} \langle p_j p\tilde{M}_{ij} \rangle} \quad (\text{B.11})$$

[Dipole 2-(5)-9t]

$$EM1'_{9t+} = e^{+i\phi(p\tilde{M}_{ij})} \frac{z_i^{(m)} \langle p_j^b p_i^b \rangle \langle p\tilde{M}_{ij} p_i^b \rangle^*}{\sqrt{2} \langle p_j^b p\tilde{M}_{ij} \rangle} \quad (\text{B.12})$$

with flat momentum

$$p_{i(j)}^b = p_{i(j)} - \frac{m_{i(j)}^2}{2p_{i(j)} \cdot p\tilde{M}_{ij}} p\tilde{M}_{ij} \quad (\text{B.13})$$

[Dipole 2-(5)-10t]

$$EM2'_+ = e^{+i\phi(p\tilde{M}_{ij})} \frac{z_i \langle p_j^b p_i^b \rangle \langle p\tilde{M}_{ij} p_i^b \rangle^*}{\sqrt{2} \langle p_j^b p\tilde{M}_{ij} \rangle} \quad (\text{B.14})$$

with

$$p_{i(j)}^b = p_{i(j)} - \frac{m_{i(j)}^2}{2p_{i(j)} \cdot p\tilde{M}_{ij}} p\tilde{M}_{ij} \quad (\text{B.15})$$

[Dipole 1-(4)-7($m_k \neq 0$) and Dipole 3-(6)-11u($m_k \neq 0$)]

$$EM3'_+ = \frac{\langle p_i p_k^b \rangle \langle p_k^b \tilde{p}_{ai} \rangle_z^*}{\sqrt{2} (1 - u_i) \langle p_i \tilde{p}_{ai} \rangle_z} \quad (\text{B.16})$$

with

$$p_k^b = p_k - \frac{m_k^2}{2p_k \cdot \tilde{p}_{ai}} \tilde{p}_{ai} \quad (\text{B.17})$$

C Comparison with the $t\bar{t} + 1\text{jet}$

	$b_0[\text{GeV}^{-4}]$	$d_0[\text{GeV}^{-4}]$
$g(p_a)g(p_b) \rightarrow t(p_t)\bar{t}(p_{\bar{t}})g(p_c)g(p_d)$		
AutoDipole	$7.82039670869613 \cdot 10^{-10}$	$1.02594003852407 \cdot 10^{-9}$
Ref. [36]	$7.82039670869604(1) \cdot 10^{-10}$	$1.02594003852396(2) \cdot 10^{-9}$
$q(p_a)\bar{q}(p_b) \rightarrow t(p_t)\bar{t}(p_{\bar{t}})g(p_c)g(p_d)$		
AutoDipole	$1.12077211361620 \cdot 10^{-10}$	$1.22619016939900 \cdot 10^{-10}$
Ref. [36]	$1.12077211361619(0) \cdot 10^{-10}$	$1.22619016939909(1) \cdot 10^{-10}$
$q(p_a)g(p_b) \rightarrow t(p_t)\bar{t}(p_{\bar{t}})g(p_c)q(p_d)$		
AutoDipole	$2.75641273146785 \cdot 10^{-11}$	$4.79768338384667 \cdot 10^{-11}$
Ref. [36]	$2.75641273146783(0) \cdot 10^{-11}$	$4.79768338384625(3) \cdot 10^{-11}$
$\bar{q}(p_a)g(p_b) \rightarrow t(p_t)\bar{t}(p_{\bar{t}})\bar{q}(p_c)g(p_d)$		
AutoDipole	$3.46150168295956 \cdot 10^{-11}$	$8.34555795894942 \cdot 10^{-11}$
Ref. [36]	$3.46150168295954(1) \cdot 10^{-11}$	$8.34555795894963(2) \cdot 10^{-11}$
$g(p_a)g(p_b) \rightarrow t(p_t)\bar{t}(p_{\bar{t}})\bar{q}(p_c)q(p_d)$		
AutoDipole	$1.21420520114780 \cdot 10^{-11}$	$2.13553289076589 \cdot 10^{-11}$
Ref. [36]	$1.21420520114779(0) \cdot 10^{-11}$	$2.13553289076550(3) \cdot 10^{-11}$
$q(p_a)\bar{q}(p_b) \rightarrow t(p_t)\bar{t}(p_{\bar{t}})\bar{q}(p_c)q(p_d)$		
AutoDipole	$5.13710959990068 \cdot 10^{-12}$	$9.06330902408356 \cdot 10^{-12}$
Ref. [36]	$5.13710959990064(1) \cdot 10^{-12}$	$9.06330902408275(3) \cdot 10^{-12}$
$u(p_a)\bar{u}(p_b) \rightarrow W^+(p_{w^+})W^-(p_{w^-})g(p_c)g(p_d)$		
AutoDipole	$0.627402537098012 \cdot 10^{-9}$	$0.114149934878320 \cdot 10^{-8}$
Ref. [40]	$0.627402537098007 \cdot 10^{-9}$	$0.114149934878319 \cdot 10^{-8}$

Table 5: The results of the $|M|^2$ and the sum of all dipole terms are shown. The two implementations agree at least to 14 digits for the matrix elements squared and at least to 12 digits for the sum of the subtraction terms. The phase space point used in the last entry corresponds to the first one in `./lib/check/check5_uux_w+w-gg/inputm_uux_w+w-gg.h`.

	c_{-2}	c_{-1}	c_0
$gg \rightarrow t\bar{t}g$			
AutoDipole	$2.49467966948003 \cdot 10^{-4}$	$3.68989776683705 \cdot 10^{-4}$	$-4.05387364353899 \cdot 10^{-4}$
Ref. [36]	$2.49467966948004(1) \cdot 10^{-4}$	$3.68989776683706(1) \cdot 10^{-4}$	$-4.05387364353900(1) \cdot 10^{-4}$
$u\bar{u} \rightarrow t\bar{t}g$			
AutoDipole	$1.38499897972387 \cdot 10^{-5}$	$2.88738914389178 \cdot 10^{-5}$	$-1.56576469322102 \cdot 10^{-5}$
Ref. [36]	$1.38499897972387(0) \cdot 10^{-5}$	$2.88738914389179(1) \cdot 10^{-5}$	$-1.56576469322102(0) \cdot 10^{-5}$
$ug \rightarrow t\bar{t}u$			
AutoDipole	$3.84580760674706 \cdot 10^{-6}$	$7.73777480040817 \cdot 10^{-6}$	$-5.19929995897616 \cdot 10^{-6}$
Ref. [36]	$3.84580760674706(0) \cdot 10^{-6}$	$7.73777480040817(1) \cdot 10^{-6}$	$-5.19929995897616(1) \cdot 10^{-6}$
$g\bar{u} \rightarrow t\bar{t}\bar{u}$			
AutoDipole	$6.22738241305372 \cdot 10^{-5}$	$6.81530745255038 \cdot 10^{-5}$	$-1.52377227863896 \cdot 10^{-4}$
Ref. [36]	$6.22738241305372(0) \cdot 10^{-5}$	$6.81530745255037(1) \cdot 10^{-5}$	$-1.52377227863896(0) \cdot 10^{-4}$

Table 6: The coefficients for the color and spin averaged results for the **I**-operator. At least 14 digits agreements are obtained.